Int. J. Electrochem. Sci., 12 **(2017)** 3088 – 3098, doi: 10.20964/2017.04.34

International Journal of
ELECTROCHEMICAL
SCIENCE
www.electrochemsci.org

Synthesis and Electrochemical Properties of Doped Tin $Fe_2(MoO_4)_3$ as Cathode Material for Sodium-Ion Batteries

Van Tu Nguyen, Yue Li Liu, Shah Abdul Hakim, Amr Rady Radwan, Bin Wei, Wen Chen[*]

State Key Laboratory of Advanced Technology for Materials Synthesis and Processing, School of Material Science and Engineering, Wuhan University of Technology, Wuhan 430070, P. R. China
[*]E-mail: chenw@whut.edu.cn

Received: 18 October 2016 / *Accepted:* 11 February 2017 / *Published:* 12 March 2017

$Fe_{2-x}Sn_x(MoO_4)_3$ samples were successfully synthesized by wet chemical route. The analytical results of X-ray diffractions indicated that the additions of tin have not destroyed the lattice structure of $Fe_{2-x}Sn_x(MoO_4)_3$, but increased the units cell volume. $Fe_{2-x}Sn_x(MoO_4)_3$ can be exhibited higher discharge /charge capacities and better cycle-stability than the pristine one. At room temperature, the initial discharge capacity of $Fe_{1.95}Sn_{0.05}(MoO_4)_3$ is 83.12 mAh g^{-1} at a discharge rate of 0.5 C and remains 78.81 after 50 cycles. The improved electrochemical properties can be explaining with the presence of tin in the lattice of $Fe_2(MoO_4)_3$ by improved the structure stability and electrical conductivity.

Keywords: NASICON. Sn doped. Iron molybdite. Cathode materials. Sodium-ion battery.

1. INTRODUCTION

The recently, many cathode materials for sodium - ion battery have been identified, such as Na_xMnO_2 [1, 2], Na_xFeO_2 [3], phostphates (olivine and sodium fluorophosphates) [4-6], NASICON compounds [7-9]. $Fe_2(MoO_4)_3$-NASICON is introduced as a potential candidate for sodium storage, but its poor cycle-stabilities and low conductivities to limits its applications [10-13]. Therefore, the approach to improve the conductivity is an important issue to be addressed precisely for its application.

Sun et al.[14] have been fabricated of nanostructure $Fe_2(MoO_4)_3$ thin films by magnetron sputtering method, and test its electrochemical properties and reaction mechanisms as cathode for sodium-ion battery. The previous our studies have been reports that $Fe_2(MoO_4)_3$ composite with nanosilver or carbon nanotubes (CNTs), reduced graphene oxide (RGO), exhibits capacity of 90 mAh

g^{-1}, and retains 84.5 % of capacity even after 50 cycles at 1 C [15-17]. The results indicated that Na^+ may be fast insertion/extraction in $Fe_2(MoO_4)_3$ nanoparticles.

Recently, one mode to meet the problems is the technical designing and improving the quality of cathode material [18-23]. Especially, doped technology in LIBs was used to improve electrochemical properties of cathode materials. Further, it can dramatically enhance mobility ion diffusions and electrons transport in the electrodes, hence improve the electrochemical properties such as large capacity and good rate cyclic stability.

For NASICON-$Li_3V_2(PO_4)_3$ material, the lows electric conductivities of $Li_3V_2(PO_4)_3$ degrades its electrochemical properties and interferes practical application. The positive effect of doping on the rate capacities and cyclic stabilities of $Li_3V_2(PO_4)_3$ have been reported in some groups of studies. Some doping methodology such as carbon coating [24-28], metal oxides coated [29] or metal ions doping [30], (Nb^{5+}, Ti^{4+}, Zr^{4+}, Fe^{3+}, Co^{2+}, Cr^{3+}, Y^{3+}, Al^{3+}, Mn^{2+}, Ce^{3+} and Mg^{2+}) that have been used successfully to doped $Li_3V_2(PO_4)_3$ [31-41]. All these doped metal ions influence the electrical conductivities and improve cycle properties of $Li_3V_2(PO_4)_3$ to different extent. Tin-doped has been shown to be favorable in some material cathode such as $LiFe_{1-x}Sn_xPO_4/C$ [42], $LiNi_{0.8}Co_{0.2}O_2$ [43], and $Li_3V_2(PO_4)_3$ [44].

For sodium-ion batteries, P2-type Na_xMO_2 (M= Mn, Fe, Co, Ni, Cr, V etc.) material, the low conductivity of Na_xMO_2 degrades its electrochemical properties and causes limited applications. Some improvements on the electrochemical performance of Na_xMO_2 have been achieved by using metal oxide coating or metal ion doping, such as Ni^{2+}, Fe^{3+}, Al^{3+}, Co^{2+}, Ca^{2+}, Mn^{2+}, and Mg^{2+} sites in Na_xMO_2 systems and carbon coating [45-51].

Tirado et al.[52] reported aluminum-doped $Na_3V_{2-x}Al_x(PO_4)_3/C$ sample was synthesized and characterized as cathode material for sodium - ion battery. The good kinetic response detected on galvanostatic cycling was explained in terms of low internal resistance at the cyclic cells. Thus, $Na_3V_{1.8}A_{l0.2}(PO_4)_3$ performed 96.8 mAh g^{-1} at 6C and preserved 103 mAh g^{-1} after decreasing to C/2 after 60 cycles.

In this paper, the monoclinic $Fe_2(MoO_4)_3$-doped tin samples have been successfully synthesized by wet chemistry. The effect of Sn^{4+}-doped on the structure and electrochemical performance are discussed in details. To the best of our knowledge, no report is available on $Fe_2(MoO_4)_3$-doped tin or their electrochemical properties as cathode materials for sodium - ion battery.

2. EXPERIMENTAL

2.1 Synthesis of $Fe_{2-x}Sn_x(MoO_4)_3$ powder

The $Fe_{2-x}Sn_x(MoO_4)_3$ was synthesized by a precipitation method as previous report [12, 15]. SnO_2 was from Sigma Aldrich (≥99.9 % purity; particle size - 325 mesh). Typically, the SnO_2 powder was dispersed in deionized water ultrasonically for eight to ten hours until to obtain a homogeneous brown solution. This solution is then added with $(NH_4)_6Mo_7O_{24}\cdot 4H_2O$ along with SnO_2 powder, followed by acidification with the nitric acid. Stoichiometric amount of $Fe(NO_3)_3\cdot 9H_2O$ solution was slowly added to the mixture solution under continuous stirring and then heated to 95-100 ^oC for 72

hours. A whole dispersion was obtained by ultrasonication for third to five hours. Finally, the precipitates were filtered, washed and calcinated at 600-650 ^{o}C for 30 hours in air. The samples with different molar ratios (0.01, 0.02, 0.05 and 0.1 M of tin) were obtained.

2.2 Fabrication of $Fe_{2-x}Sn_x(MoO_4)_3$ electrodes

Fabrication of $Fe_{2-x}Sn_x(MoO_4)_3$ electrodes were prepared as our previous report [15-17]. The working electrodes were prepared by spreading the slurry of the $Fe_{2-x}Sn_x(MoO_4)_3$ (80 wt%), acetylene black (15 wt%), and binder polytetrafluoroethylene (PTFE) (5 wt%) on Ni mesh. The electrodes were dried at 100^{o}C in vacuum for eight to ten hours prior to use. The electrochemical performances were investigated in CR2025 coin type cell with metal sodium foils as the anode electrodes. The $NaClO_4$ (Aldrich, 99.99 wt.%) and propylene carbonate solvent (PC, Aladdin, China) were used as electrolytes (1 mol/L). Micro-porous film (polypropylene, Cellgard 2300) was used as a separator. All cells were assembled in an argon-filled glove box at room temperature.

2.3 Characterization and measurements

The crystalline structures of samples were characterized by X-ray diffractometer (XRD, PertrPro PANalytical, Netherlands) equipped with Cu Kα radiation (1.5418Å). The morphologies of the samples were measurements by the scanning electron microscope (SEM, JSM-6700F, JEOL, Tokyo, Japan). X-ray photoelectron spectroscopy (XPS) measurements were used by VG Multilab 2000, with Al Kα the as the radiation source and all XPS spectra were corrected by the C_{1s} line at 284.8 eV. The Brunauer-Emmett-Teller (BET) specific surface area of powders were analyzed in a nitrogen adsorption-desorption apparatus by TriStar II 3020 (Micrometrics, American).

2.3.1 Electrochemical measurements

The galvanostatic discharge/charge tests were carried out on a battery test system (Land BT2000, Wuhan, China). The cyclic voltammetry (CV) and electrochemical impedance spectroscopies (EIS) were measurements by Autolab Potentiostat (Potentiostat 30, Metrohm Autolab, Netherlands).

3. RESULTS AND DISCUSSION

3.1 Structural and morphological characterization

The X-ray diffraction (XRD) patterns of $Fe_{2-x}Sn_x(MoO_4)_3$ (x = 0, 0.01, 0.02, 0.05 and 0.10) compounds are presented in Fig. 1. All samples were seen to be single phase, and did not see the presence of impurities can be finding within the resolution of our diffractmeter. It means that SnO_2 is no presence and has been doped into $Fe_2(MoO_4)_3$. The XRD patterns of $Fe_{2-x}Sn_x(MoO_4)_3$ compounds were successfully indexed with a monoclinic lattice using the program Jade 6.5. The unit cell lattices parameters of the experimental $Fe_{2-x}Sn_x(MoO_4)_3$ phases are shown in Table 1. It can be seeing that,

after Sn doping, the lattices increase with increasing the Sn contents. The changes give rise to increase the volume of unit cell; it may enhance Na^+ ions mobility.

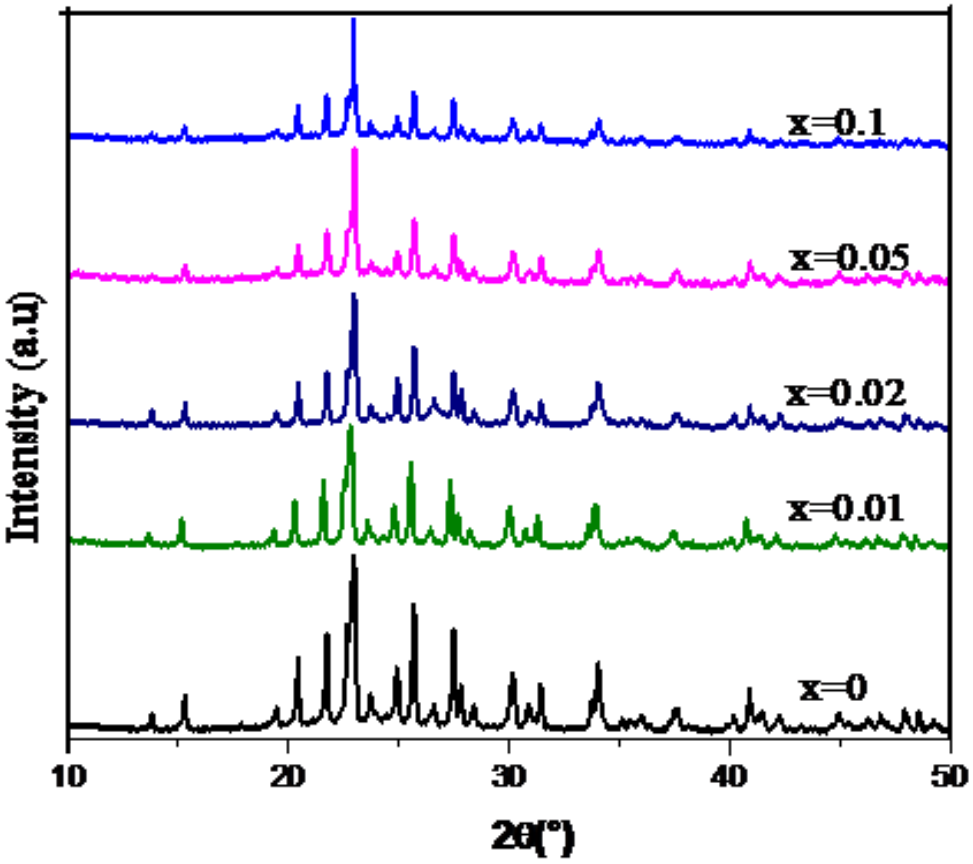

Figure 1. XRD patterns of $Fe_{2-x}Sn_x(MoO_4)_3$ compounds

Table 1. Refined unit cell lattices parameters for $Fe_{2-x}Sn_x(MoO_4)_3$ cells (x = 0, 0.01, 0.02,0.05, 0.10).

x	a(Å)	b (Å)	c (Å)	β (°)	V(Å^3)
0.0	15.6945	9.2361	18.2345	125.539	2148.65
0.01	15.7195	9.2372	18.2203	125.453	2154.65
0.02	15.7217	9.2389	18.2134	125.425	2155.68
0.05	15.7591	9.2432	18.2094	125.587	2172.32
0.10	16.0546	9.3220	18.2090	125.699	2255.36

The SEM images of the $Fe_{2-x}Sn_x(MoO_4)_3$ (x = 0, 0.01, 0.02, 0.05 and 0.10) samples are shown in Fig. 2. As see in Fig. 2, the particles of 0.1-1μm size and aggregate structure can be seen for $Fe_2(MoO_4)_3$ samples (Fig. 2a), while the $Fe_2(MoO_4)_3$-Sn doped samples have a smaller particles size

(Fig. 2b-e). The results indicates that the additions of tin may be affected the morphologies of samples. For small sized particles capable of contact between cathode materials and electrolytes, this is favorable for the diffusion and transmission of Na^+ ion in the electrodes [45].

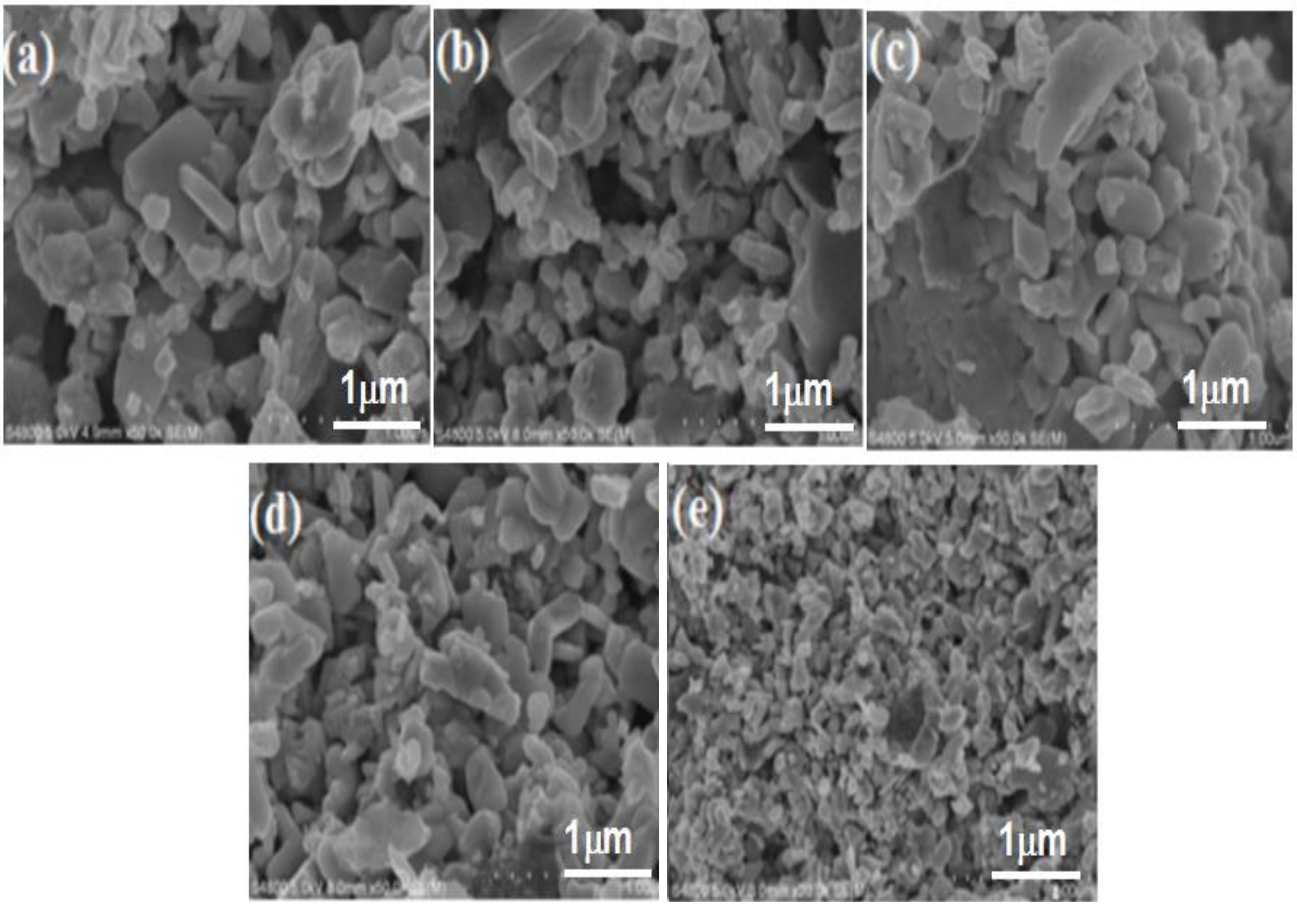

Figure 2. SEM image of $Fe_{2-x}Sn_x(MoO_4)_3$ samples with different Sn contents (a) x = 0; (b) x=0.01; (c) x= 0.02; (d) x= 0.05 and (e) x=0.10.

The specific surface area of $Fe_{1.95}Sn_{0.05}(MoO_4)_3$ and $Fe_2(MoO_4)_3$ powder have been estimated to be 1.65 $m^2\ g^{-1}$ and 1.63 $m^2\ g^{-1}$, respectively. This result indicates specific surface area between $Fe_{1.95}Sn_{0.05}(MoO_4)_3$ and $Fe_2(MoO_4)_3$ changes small.

Fig. 3 shows the XPS results of $Fe_{2-x}Sn_x(MoO_4)_3$ powders. The XPS peak of Sn3d in Fig. 3b is about 487.16 eV and in accordance with the valence four of tin, doping materials previous reported [46]. Fig. 3c depicts the Fe2p XPS core level for $Fe_2(MoO_4)_3$ and $Fe_{1.95}Sn_{0.05}(MoO_4)_3$. The spectra of Mo3d in Fig. 3d show the characteristic peak of Mo^{6+} state located at 232.8 eV. Further, for samples with doped and undoped tin have not alter characteristic peaks of Fe2p and Mo3d (711.79 and 232.8 eV, respectively), which means that the doping tin does not change the state of Fe^{3+} and Mo^{6+} in $Fe_2(MoO_4)_3$.

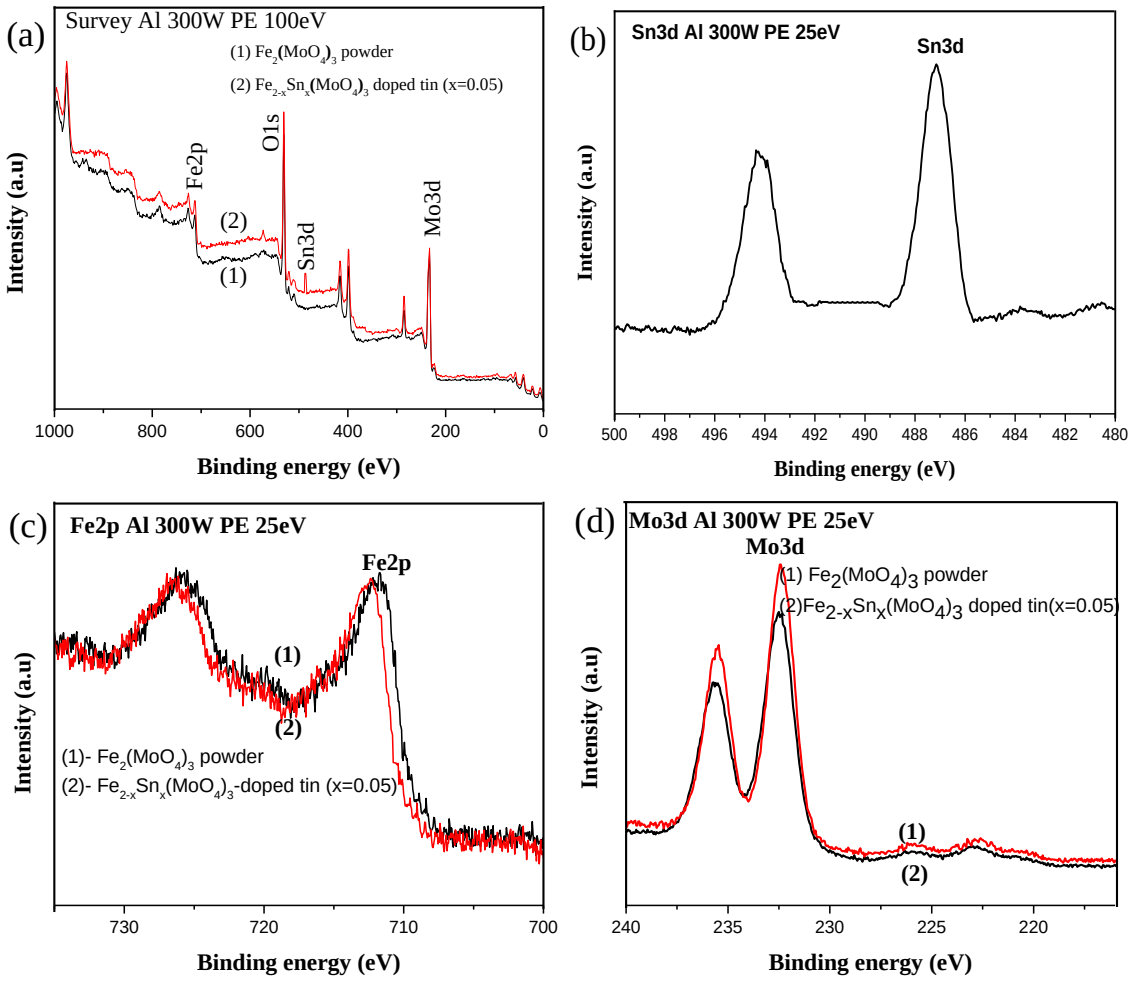

Figure 3. X-ray photoelectron spectra of $Fe_2(MoO_4)_3$ powder and $Fe_{1.95}Sn_{0.05}(MoO_4)_3$. (a) Survey spectra; (b) Sn3d spectrum; (c) Fe2p spectra; (d) Mo3d spectra.

3.2 Electrochemical performance of $Fe_{2-x}Sn_x(MoO_4)_3$

The first cyclic voltammetry curves of the $Fe_{2-x}Sn_x(MoO_4)_3$ electrodes between 1.5 and 3.5 V at scan rate of 0.1 mV s^{-1} shown in Fig. 4a. Some distinct features are as follows. (i) Two peaks of cathode and anode in cells indicate insertion/extraction of Na^+ ion in the electrode. The curves of $Fe_{2-x}Sn_x(MoO_4)_3$ shows higher peaks which indicate higher current change compared to $Fe_2(MoO_4)_3$ powder. (ii) The cyclic voltammetry of $Fe_{2-x}Sn_x(MoO_4)_3$ exhibits the cyclability and reversibility of all cycles.

Two cathode peaks at 2.625(φ_{op}) and 2.525 V and anodic peaks at 2.55(φ_{Rp}) and 2.715 V are observed in the first redox process for $Fe_{1.95}Sn_{0.05}(MoO_4)_3$. The cathode peaks of $Fe_{1.95}Sn_{0.05}(MoO_4)_3$ are larger than those of $Fe_2(MoO_4)_3$. And the anode peaks of $Fe_{1.95}Sn_{0.05}(MoO_4)_3$ are smaller than those of $Fe_2(MoO_4)_3$. The potential difference, ΔE (φ_{op}- φ_{Rp}) between anode and cathode peaks can indicate the polarization degree of electrode [45, 46]. The potential differences (ΔE) of all $Fe_{2-x}Sn_x(MoO_4)_3$ are lower than those of $Fe_2(MoO_4)_3$ electrodes. It suggests that the reversibility properties of Fe_{2-}

$_xSn_x(MoO_4)_3$ is significantly improved. The results are appropriate with the cycling profiles and indicates a reversible two-step electrochemical reaction mechanisms of $Fe_2(MoO_4)_3$ with sodium ions.

Fig. 4b shows the first charge/discharge profiles of $Fe_{1.95}Sn_{0.05}(MoO_4)_3$/Na cell at current rates of 0.1 C (9 mA g^{-1}), 0.2 C (18 mA g^{-1}), 0.3 C (27 mA g^{-1}) and 0.5 C (45 mA g^{-1}) in the potential of 1.8-3.5 V (vs Na/Na^+). At a current rate of 0.1 C, the charge/discharge capacities of $Fe_{1.95}Sn_{0.05}(MoO_4)_3$ are about 89.5 and 90.3 mAh g^{-1}, respectively, corresponding to about 2.0 Na^+ per formula unit (p.f.u), which implies that the Fe^{3+} highly transforms to Fe^{2+}. It is major reason to increase specific capacity of the $Fe_{1.95}Sn_{0.05}(MoO_4)_3$.

The electrochemical performances of $Fe_2(MoO_4)_3$ powder and the $Fe_{1.95}Sn_{0.05}(MoO_4)$ (x=0.05) in Na half-cells are compared in Fig. 4c. All gravimetric capacities of $Fe_{1.95}Sn_{0.05}(MoO_4)_3$ is calculated based on the total weight of the material, which contains about 9.97 wt.% tin. Fig. 4c also clearly shows the corresponding specific capacities of $Fe_{1.95}Sn_{0.05}(MoO_4)_3$ as a function of cycle number at 0.1 C, 0.2 C, 0.3 C and 0.5 C, respectively. Although two samples are similar crystalline and same $Fe_2(MoO_4)_3$ phase, however, the high rate performances for the two samples are entirely different. $Fe_{1.95}Sn_{0.05}(MoO_4)_3$ delivers the discharge capacities of 90.5, 87.76, 85.60, and 83.12 mAh g^{-1} at 0.1; 0.2; 0.3 and 0.5 C, respectively, while $Fe_2(MoO_4)_3$ powders delivers the discharge capacity of 80.10 mAh g^{-1} at 0.1C. The results show that the discharge capacity of the $Fe_2(MoO_4)_3$ powder electrodes decreases rapidly, although it exhibits a discharge capacity of 80 mAh g^{-1} in the first cycle, only around 20 mAh g^{-1} remains after 30 cycles at low rate of 0.1 C. Apparently, the $Fe_{1.95}Sn_{0.05}(MoO_4)_3$ electrodes shows a larger capacity and better cyclic stability than the $Fe_2(MoO_4)_3$ powder electrodes. For at high rate (0.5C), it is still able to deliver stable capacity of 83.12 $mAhg^{-1}$, and it is maintained 91.85 % of theoretical capacity. The improved specific capacities and good discharge at high rate of the $Fe_{1.95}Sn_{0.05}(MoO_4)_3$ sample may be related to its refined unit cell lattice parameters, which may facilitate the diffusion process. While the increasing of current rate, especially at high current, the discharge voltage decreases and the charge voltage increases due to the effect of increasing electrochemical polarization. This is further studied by electrochemical impedance spectroscopy method.

Fig. 4d shows the Nyquist plots of $Fe_2(MoO_4)_3$ and $Fe_{1.95}Sn_{0.05}(MoO_4)_3$ cathode after three cycles at 9 mA g^{-1} in the frequency range between 100 kHz and 0.1 Hz at open circuit voltage (OCV) with 5 mV amplitude voltage. The semicircles at high to medium frequency are mainly related to a complex reaction process at the electrolyte/cathode interface. The inclined line in the lower frequency region is attributed to the Warburg impedance, which is associated with sodium-ion diffusion in the $Fe_2(MoO_4)_3$ electrode. It can be observed that the diameter of the high-frequency-combined semicircle of $Fe_{1.95}Sn_{0.05}(MoO_4)_3$ is smaller than that of the $Fe_2(MoO_4)_3$ powders. In impedance spectra fitted using an equivalent circuits, R_e represents the total resistance of electrolytes, electrode and separators. R_f and CPE1 are related to the diffusion resistance of Na^+- ions through the solid electrolytes interfaces (SEI) layer and the corresponding constant phase element (CPE). R_{ct} and CPE2 correspond to the charge transfer resistance and the corresponding CPE. Z_w is Warburg impedance [15]. The exchange current density is calculated using the following equation.

$$i^o = RT/nFR_{ct}$$

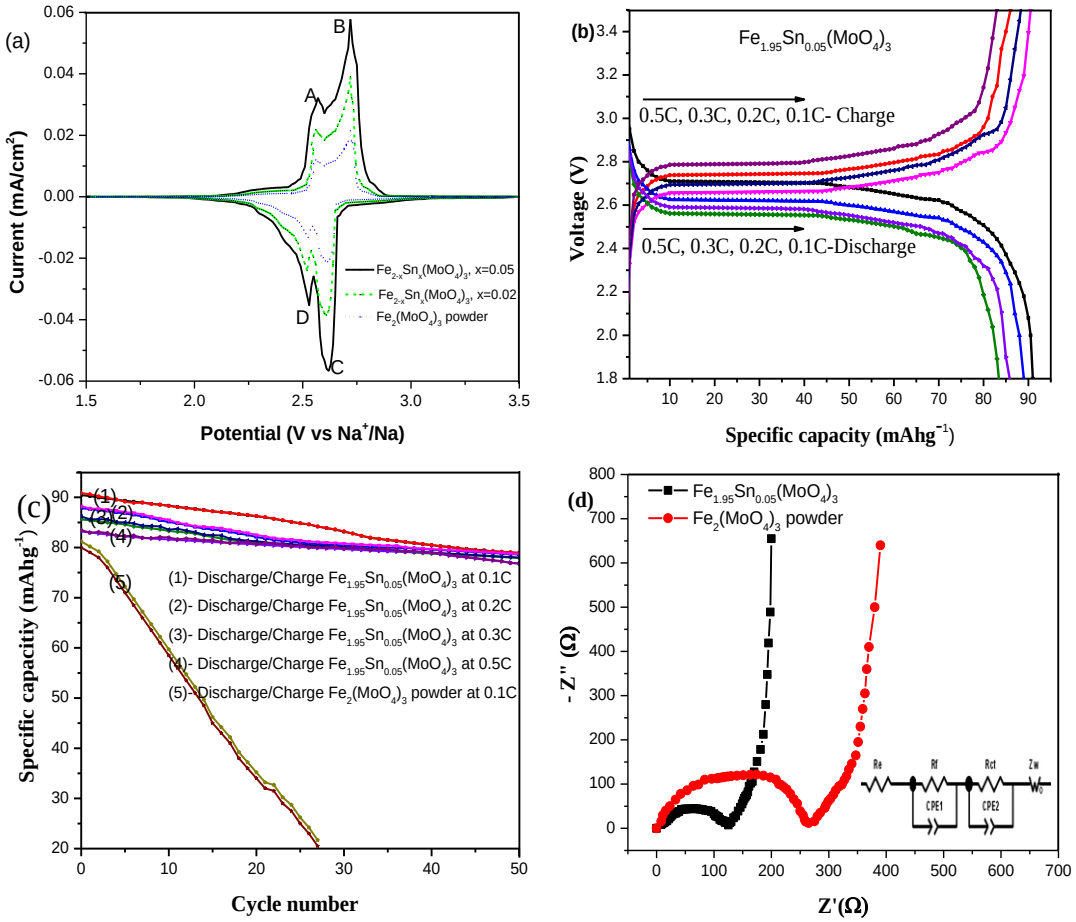

Figure 4. (a) The first cyclic voltammetry curves of $Fe_{2-x}Sn_x(MoO_4)_3$ electrode at a voltage sweep rate of 0.1 mV s^{-1}; (b) Galvanostatic curves of $Fe_{1.95}Sn_{0.05}(MoO_4)_3$/Na cell at a current rates of 0.1, 0.2, 0.3 and 0.5C; (c) The specific capacities of $Fe_{2-x}Sn_x(MoO_4)_3$ 0.1, 0.2, 0.3 and 0.5 C and $Fe_2(MoO_4)_3$ powders at 0.1C; (d) EIS plots of $Fe_2(MoO_4)_3$ and $Fe_{1.95}Sn_{0.05}(MoO_4)_3$ powders after 3 cycles at 9 mA g^{-1} in the frequency range between 100 kHz and 0.1 Hz at open circuit voltage (OCV) with 5mV amplitude voltage (Inset shows the equivalent circuits corresponding to the Nyquist plots).

The fitting results of R_e, R_f, R_{ct} and i_o as shown in Table 2. It indicated the R_f and R_{ct} values of $Fe_{1.95}Sn_{0.05}(MoO_4)_3$ cathode are smaller than that of $Fe_2(MoO_4)_3$ powder, as the $Fe_{1.95}Sn_{0.05}(MoO_4)_3$ show the lowest resistance and the largest exchange current density, it suggests that $Fe_2(MoO_4)_3$ sample doped tin significantly improves the performance of the sodium-ion batteries. This results can be indicated that the decreased of charge-transfer resistance is beneficial to insert/extraction ion Na^+ easily, so the kinetic behaviors during discharge/charge processes.

Table 2. Impedance parameters calculated from equivalent circuits.

Sample	R_e (Ω)	R_f (Ω)	R_{ct} (Ω)	i^o (mA cm^{-2})
$Fe_2(MoO_4)_3$ powder	10.55	120.86	265.60	4.831×10^{-5}
$Fe_{1.95}Sn_{0.05}(MoO_4)_3$	9.5	62.01	100.08	1.273×10^{-4}

Table 3, the specific capacity of $Fe_{1.95}Sn_{0.05}(MoO_4)_3$ is compared with previous results, it is decreased little (at rates 0.1 C and 0.2 C). But it advantages by the synthetic aspects and low cost.

Table 3. The specific capacity of $Fe_2(MoO_4)_3$ as the cathode material for SIBs.

Samples	*n electron transitions*	*Open circuit voltage V vs. Na*	C ($mAhg^{-1}$)	Rate current	Ref
$Fe_2(MoO_4)_3$ powder	~1,8	~2,6	82.0	0.01 C	[12, 13, 53, 55]
$Fe_2(MoO_4)_3$ nano (thin films)	2	~2,6	91.0	1 C	[14]
$Fe_2(MoO_4)_3$/nano silver	2	~2,6	90.2	0.1 C	[15]
$Fe_2(MoO_4)_3$ /CNTs	2	~2,6	85.6	1 C	[16]
$Fe_2(MoO_4)_3$ /RGO	2	~2,6	90.1	1 C	[17]
$Fe_2(MoO_4)_3$ /RGO	2	~2,6	89.0	2 C	[54]
$Fe_{1.95}Sn_{0.05}(MoO_4)_3$	~2	~2,6	87.8	0.2 C	This works

4. CONCLUSIONS

$Fe_{2-x}Sn_x(MoO_4)_3$ samples were successfully prepared by wet chemical route, which the addition of tin do not destroy the lattice structure of $Fe_{2-x}Sn_x(MoO_4)_3$, but increases the unit cell volume. As a cathode material of sodium-ion, $Fe_{1.95}Sn_{0.05}(MoO_4)_3$ exhibits the best capacity that the initial capacity is 83.12 mAh g^{-1}, and remains 78.81 mAh g^{-1} after 50 cycles. The improved capacity of $Fe_{1.95}Sn_{0.05}(MoO_4)_3$ may be related to its refined unit cell lattice parameters, which induces the mobility for both Na^+ ion diffusion and electron transports. The $Fe_{2-x}Sn_x(MoO_4)_3$ samples significantly improve conductivity and refined unit cell lattice parameters, which causes the advancement in the performance of the sodium- ion batteries.

ACKNOWLEDGMENTS
This work is supported by the National Nature Science Foundation of Hubei Province (No. 2014CFB165), Science and Technology Support Program of Hubei Province (No. 2014BAA096), Equipment pre-research project (No. 625010402), and the International S&T Cooperation program of China (ISTCP) (No. 2013DFR50710).

References

1. M. D. Slater, D. H. Kim, E. Lee and C. S. Johnson, *Adv. Funct. Mater.*, 23 (2013) 947
2. M. M. Doeff, Y. P. Ma, M. Y. Peng, and L. D. Jonghe, *J. Electrochem. Soc.*, 141 (1994) L145
3. J. Molenda, C. Delmas and P. Hagenmuller, *Solid State Ionics*, 9 - 10 (1983) 431
4. K. Chihara, A. Kitajou, I. D. Gocheva, S. Okada and J. Yamaki, *J. Power Source*s 227 (2013) 80
5. V. Palomares, M. Casas-Cabanas, E. Castillo-Martinez, M. H. Han and T. Rojo, *Energy Environ. Sci.*, 6 (2013) 3212.
6. R. K. B. Gover, A. Bryan and P. Burns, *Solid State Ionics*, 177 (2006) 1495

7. B. L. Ellis and F. N. Linda, *Solid State & Materials Science,* 16 (2012) 168
8. Z. L. Jian, L. Zhao, H. L. Pan, Y. S. Hu, H. Li, W. Chen and L. Q. Chen, *Electrochem. Commun*., 14 (2012) 86
9. N. Yabuuchi, K. Kubota, M. Dahbi and S. Komaba, *Chem. Rev.*, 114 (2014) 1636
10. K. S. Nanjundaswamy, A. K. Padhi, J. B. Goodenough, S. Okada, H. Ohtsuka, A. Arai and J. Yamaki, *Solid State Ionics*, 92 (1996) 1
11. A. Manthiram and J. B. Goodenough, *J. Solid State. Chem.*, 71 (1987) 349
12. P. G. Bruce and G. Miln, *J. Solid State Chem.*, 89 (1990) 162
13. J. Shirakawa, M. Nakaya, M. Wakihar and Y. Uchimoto, *J. Phys. Chem.* B, 11 (2007) 1424
14. Q. Sun, Q. Q. Ren and Z.W. Fu, *Electrochem. Commun.,* 23 (2012) 145
15. V. T. Nguyen, Y. L. Liu, X. Yang and W. Chen, *ESC Electrohem. Lett*., 4(1) (2015) A32
16. V. T. Nguyen, Y. L. Liu, S. A. Hakim, X. Yang, Yang Li and W. Chen, *ECS J. Solid State Sci. Technol.*, 4(5) (2015) M25.
17. V.T. Nguyen, Y. L. Liu, S. A. Hakim, S. Yang, A. M. Radwan and W. Chen, *Int. J. Electrochem. Sci.,* 10 (2015) 1065
18. J. Xie, N. Imanishi, T. Zhang, A. Hirano, Y. Takeda, O. Yamamoto, X. B. Zhao and G. S. Cao, *J. Power Sources*, 195 (2010) 8341
19. K. Du, R. Kwang-Sun, D. H. Huang and G. R. Hu, *J. Power Sources*, 238 (2013) 372
20. L. J. Jacob, J. T. Hung and Y. T. Meng, *J. Power Sources*, 189 (2009) 702
21. T. F.Yi, X. Y. Li, H. P. Liu, J. Shu, Y. Zhu and R. S. Zhu, *Ionics*, 18 (2012) 529
22. J. Barker, M. Y. Saidi and J. Swoyer, *J. Electrochem. Solid State Lett.,* 6 (2003) A1
23. N. Tatsuya, M. Yoshiki, T. Mitsuharu and Y. Yoshihiro, *J. Electrochem. Soc.,* 153 (2006) A1108
24. C. Chang, J. Xiang, X. Shi, X. Han, L. Yuan and J. Sun, *Electrochim. Acta,* 54 (2008) 623
25. Y. Q. Qiao, J. P. Tu, Y. J. Mai, L. J. Cheng, X. L. Wang and C.D. Gu, *J. Alloys Compd*., 509 (2011) 7181
26. Y. Q. Qiao, X. L. Wang, Y. J. Mai, J. Y. Xiang, D. Zhang, C. D. Gu and J. P. Tu, *J. Power Sources*, 196 (2011) 8706
27. T. Jiang, W. Pan, J. Wang, X. Bie, F. Du, Y. Wei, C. Wang and G. Chen, *Electrochim. Acta,* 55 (2010) 3864
28. Y. Q. Qiao, X. L. Wang, Y. J. Mai, X. H. Xia, J. Zhang, C. D. Gu and J. P. Tu, *J. Alloys Compd.*, 536 (2012) 132
29. J. Zhai, M. Zhao, D. Wang and Y. Qiao, *J. Alloys Compd.*, 502 (2010) 401
30. L. Zhang, Y. Li, G. Peng, Z. Wang, J. Ma, W. Zhang, X. Hu and Y. Huang, *J. Alloys Compd.*, 513 (2012) 414
31. Q. Kuang, Y. Zhao, X. An, J. Liu, Y. Dong and L. Chen, *Electrochim. Acta*, 55 (2010) 1575
32. Y. P. Wu, E. Rahm and R. Holze, *Electrochim. Acta,* 47 (2002) 3491
33. M. Ren, Z. Zhou, Y. Li, X. P. Gao and J. Yan, *J. Power Sources,* 162 (2006) 1357
34. D. Ai, K. Liu, Z. Lu, M. Zou, D. Zeng and J. Ma, *Electrochim. Acta*, 56 (2011) 2823
35. Y. Chen, Y. Zhao, X. An, J. Liu, Y. Dong and L. Chen, *Electrochim. Acta,* 54 (2009) 5844
36. Y. Xia, W. Zhang, H. Huang, Y. Gan, C. Li and X. Tao, *Mater. Sci. Eng.* B, 176 (2011) 633
37. Y. Z. Dong, Y. M. Zhao and H. Duan, *J. Electroanal. Chem.,* 660 (2011) 14
38. T. Zhai, M. Zhao and D. Wang, *Trans. Nonferr. Metal Soc.*, 21 (2011) 523
39. J. Barker, R. Gover, P. Burns and A. Bryan, *J. Electrochem. Soc*., 154 (2007) A307
40. S. Zhong, L. Liu, J. Jiang, Y. Li, J. Wang, J. Liu and Y. Li, *J. Rare Earth*, 27 (2009) 134
41. J. Yao, S. Wei, P. Zhang, C. Shen, K. A. Zinsou and L. Wang, *J. Alloys Compd.,* 532 (2012) 49
42. J. Ma, B. Li, H. Du, C. Xu and F. Kang, *Electrochim. Acta*, 56 (2011) 7385
43. X. Ma, C. Wang, J. Cheng and J. Sun, *Solid State Ionics*, 178 (2007) 125
44. H. P. Liu, S. F. Bi, G. W. Wen, X. G. Teng, P. Gao, Z. J. Ni, Y. M. Zhu and F. Zhang, *J. Alloys Compd.,* 543 (2012) 99
45. D. Kim, E. Lee, M. D. Slater, W. Lu and C. S. Johnson. *Electrochem. Commun.,* 18 (2012) 66

46. V. N. Nguyen, P. W. Ou and Ming Hung. *Ceramics International*, 41 (2015) 10199
47. H. Yoshida, N. Yabuuchi and S. Komaba. *Electrochem. Commun.*, 34 (2013) 60.
48. N. Bucher, H. Steffen, J. B. Franklin, M. W. Anna, Y. L. Linda, H. Y. Chen, N. W. Johanna, F. T. Michael and S. Madhavi. *Chem. Mater.*, 28 (2016) 2041
49. S. C. Han, H. Lim, J. Y. Jeong, D. Ahn, W. B. Park, S. K. Sun and M. H. Pyo. *J. Power Sources*, 277 (2015) 9
50. D. D. Yuan, X. H. Hu, J. F. Qian and Y L. Cao. *Electrochim. Acta*, 116 (2014) 300
51. D. Buchholz, V. Christoph, G. C. Luciana and P. Stefano. *J. Power Sources*, 282 (2015) 581
52. M. J. Aragón, P. Lavela, R. Alcántara and J. L. Tirado. *Electrochim. Acta*, 180 (2015) 824
53. J. L. Yue, Y. N. Zhou, S.Q. Shi, Z. Shadike, X. Q. Huang, J. Luo, Z. Z. Yang, H. Li, L. Gu, X. Q. Yang and Z. W. Fu. *Scientific Reports*, 5 (2015) 8810, DOI: 10.1038/srep08810
54. J. Z. Sheng, H. Zang, C. J. Tang, Q. Y. An, Q. L. Wei, G. B. Zhang, L. N. Chen, P. Chen and L. Q. Mai. *Nano Energy*, 24 (2016) 130
55. S.L. Zhou, B. Gozde, M. J. Benjamin, B. C. Melot and R. L. Brutchey. *Chemistry of Materials*, 28 (12) (2016) 4492